

## Direct Diagnoses of Stratosphere–Troposphere Exchange

ANDREW GETTELMAN AND ADAM H. SOBEL

*Department of Atmospheric Sciences, University of Washington, Seattle, Washington*

(Manuscript received 31 July 1998, in final form 17 February 1999)

### ABSTRACT

This study discusses the direct diagnosis of stratosphere–troposphere exchange. The method introduced by Wei is applied to the Goddard Earth Observation System assimilated dataset. In many respects, the results generally agree with those of other studies using the same method and different datasets. However, sensitivity tests and theoretical considerations indicate that the instantaneous two-way exchange may be significantly exaggerated by the Wei method, because the method is rather sensitive to input data errors such as those that are invariably present in assimilated datasets. The method becomes somewhat better conditioned as the results are more heavily averaged, but this also reduces the method's ability to diagnose two-way exchange. Additionally, when the flux across various surfaces is averaged over the globe and the entire year, the result implies unrealistically large imbalances in the annually averaged mass budget of the stratosphere. This could be caused by modest biases in the model used to perform the data assimilation. Since pure model simulations have an internal dynamical consistency that is lacking in assimilated datasets, the analysis appears to explain the fairly large discrepancies between the two-way fluxes obtained in studies using models and those obtained in studies using assimilated datasets. It may also explain the discrepancies between the net fluxes obtained by the Wei method and those obtained by other methods.

### 1. Introduction

In order to understand the physics and chemistry of the upper troposphere and lowermost stratosphere, quantitative information on the mass and property transports between these two regions is required. While important aspects of the circulation of mass between the troposphere and the region of the middle atmosphere known as the “overworld” (Shaw 1930; Hoskins 1991) are fairly well constrained (Holton et al. 1995), this does not imply a similar level of certainty concerning actual property fluxes across the tropopause. Recently, several studies have performed calculations intended to remedy this lack of quantitative knowledge, using the method described by Wei (1987, hereafter the “Wei method”). This method, in principle, allows both upward and downward components of the cross-tropopause mass flux to be separately determined. Some other commonly used methods only constrain the net mass flux, which is in general inadequate to determine fluxes of chemical species. This study applies the Wei method to assimilated fields from the Goddard Earth Observation System (GEOS) dataset. One aim is to provide results for comparison with similar calculations using other datasets. A second aim is to perform calculations that test the

robustness of the Wei method, particularly when a typical global assimilated dataset is used and quantitative results are desired. We find that while the method is a useful tool for some purposes, it places severe demands on the quality of the input data. Because of this, the method may be ill conditioned in practice when used to obtain quantitative results from data of realistic quality. Our analysis suggests that better results might be expected when the diagnostic is applied to output from free-running model simulations, but, in fact, problems similar in nature to those discussed here are reported by Wirth and Egger (1999) even with a free-running model.

Throughout this paper we will use the term cross-tropopause flux (CTF) to refer to the exchange of mass across a surface defined as separating the stratosphere and troposphere. The CTF may be instantaneous or averaged. Where appropriate, we will specify what type of averaging, if any, has been applied; if no averaging is mentioned, instantaneous CTF is meant. The CTF may be reversible, in the sense that an air parcel may cross the surface in one direction and then cross back again soon after, without undergoing true mixing.

We first describe conceptual issues related to two-way exchange and the results of previous studies in section 2. We then describe our implementation of the Wei method in section 3 and present results from these calculations in section 4. The results are broken into a discussion of mass budgets in section 4a, instantaneous snapshots in section 4b, monthly integrated results in

---

*Corresponding author address:* Dr. Andrew Gettelman, NCAR/ASP Program, P.O. Box 3000, Boulder, CO 80307-3000.  
E-mail: andrew@ucar.edu

section 4c, and globally and annual integrated results in section 4d. We discuss the effect of errors in the input data in section 5 and present conclusions in section 6.

## 2. Basic concepts and results of previous studies

Consider a two-dimensional surface defining the tropopause. At every point on the surface the mass flux across it per unit surface area can be written:

$$\tilde{m} = \rho(\mathbf{u} - \mathbf{u}_c) \cdot \hat{\mathbf{n}}, \quad (1)$$

where  $\mathbf{u}$  is the three-dimensional fluid velocity,  $\mathbf{u}_c$  is the velocity of the surface itself,  $\rho$  is the density, and  $\hat{\mathbf{n}}$  is the unit vector normal to the surface. As is typical in previous studies, we will for most purposes use the quantity

$$m = \frac{\tilde{m}}{\cos\alpha}, \quad (2)$$

where  $\alpha$  is the angle between  $\hat{\mathbf{n}}$  and the vertical, assumed less than  $90^\circ$ ; and  $m$  is the mass flux across the surface per unit horizontal area rather than per unit surface area. When the surface is the tropopause (however defined) we will call  $m$  the ‘‘instantaneous CTR’’

The Wei method is equivalent in principle to the direct application of (1) and (2). The more complex expressions in Wei’s paper result from taking the surface to be an isosurface of potential vorticity (PV) and expanding the terms, resulting in expressions such as (5) below. More detailed presentations of the manipulations involved can be found in Wei (1987) and Wirth and Egger (1999).

In some studies, the instantaneous, local mass flux  $m(x, y, t)$  is presented only after having been submitted to some integration or averaging, in time as well as either zonally or over large areas. While this may be instructive, it obscures the information that is most directly relevant for making inferences about the fluxes of material properties, such as trace gases, since these depend directly on the extent to which a given net mass flux is made up of canceling components of opposite sign.

To understand the two-way aspects of stratosphere–troposphere exchange, we can integrate the positive and negative components of  $m(x, y, t)$  separately. That is, we can integrate over longitude, time, etc., but perform the integral twice, first including only points where  $m$  is positive, and then only those where it is negative. Call the resulting upward and downward integrated mass fluxes  $M_u$  and  $M_d$ , respectively, with the sign built into the definition so that both are positive numbers. These  $M_u$  and  $M_d$  will be collectively referred to hereafter as ‘‘gross’’ fluxes. The net mass flux is simply the difference of these,

$$M = M_u - M_d,$$

where we have defined positive upward.

The relevance of  $M_d$  and  $M_u$  to tracer fluxes is most

easily illustrated by considering the idealized case of a trace gas,  $q$ , which has uniform mixing ratio  $q_1$  just below the tropopause and  $q_2$  just above, with a discontinuity at the tropopause. In this case, the flux of  $q$  across the surface is

$$F_q = M_u q_1 - M_d q_2. \quad (3)$$

There is no way to infer  $F_q$  from the total mass flux  $M$  alone. Equation (3) can be rewritten

$$F_q = M q_2 + M_u (q_1 - q_2), \quad (4)$$

so that in this case the flux of tracer has a one-way part, which depends only on the tracer mixing ratio above the tropopause, and a two-way part, which depends on the difference in the mixing ratios above and below the tropopause and is zero if  $M_u = 0$ .

Downward control theory (Haynes et al. 1991; Holton et al. 1995) and radiatively derived estimates of the residual circulation (Rosenlof 1995; Eluszkiewicz et al. 1996) do not provide any direct information on tracer fluxes, because they constrain only  $M$ . Additional assumptions, such as taking  $M_u = 0$  at some surface well above the tropopause, can make  $M$  useful for analyzing the cross-tropopause fluxes of long-lived constituents, provided the chemical lifetimes of the constituents are longer than the transit time through the region between the chosen upper surface and the tropopause. In that case the cross-tropopause tracer flux is computed as a residual from the total budget of tracer for that intervening region. This approach has been used to calculate the cross-tropopause flux of ozone using the zonally and temporally averaged residual circulation (Gettelman et al. 1997) and using transport models (Lelieveld and Crutzen 1994; Tie and Hess 1997). For shorter-lived species, this approach is invalid.

The major advantage of the Wei method, then, is that in principle it allows the direct computation of  $M_u$  and  $M_d$ . Spaete et al. (1994), Lamarque and Hess (1994), Siegmund et al. (1996), and Wirth and Egger (1999) have separately computed  $M_u$  and  $M_d$  using the Wei method or variants of it. The four studies used different datasets. Lamarque and Hess (1994) and Spaete et al. (1994) used mesoscale model simulated data over regional domains and periods of four days and one day respectively, while Siegmund et al. (1996) used forecast data from the European Centre for Medium-Range Weather Forecasts (ECMWF) for the extratropical Northern Hemisphere for an entire month. Wirth and Egger (1999) used ECMWF GCM model data over a regional domain for three days. For these studies the values of the ratio  $M_u/M_d$  were 0.24 (Wirth and Egger 1999), 0.4 (Spaete et al. 1994), 0.79 (Lamarque and Hess 1994), and 0.97 (Siegmund et al. 1996). The spread in these values, a factor of 4, implies widely differing patterns of stratosphere–troposphere exchange in the different studies. When  $M_u/M_d$  is close to unity, it implies that the exchange is mostly two-way, with the net mass flux  $M$  being a small residual of much larger up-

ward and downward fluxes. When the same ratio is small compared to unity, it implies a more nearly one-way transport, so that tracer fluxes will be to a greater extent determined by the net mass flux  $M$  [see Eq. (4)]. This effect can alternately be quantified by the ratio  $M_u/M$ , which measures the relative importance of the second term in (4) relative to the first, in the case  $q_1 = 0$  (a reasonable first approximation for, e.g., ozone). For the above-mentioned studies this ratio is  $-0.3$  (Wirth and Egger 1999),  $-0.67$  (Spaete et al. 1994),  $-3.67$  (Lamarque and Hess 1994), and  $-32.33$  (Siegmund et al. 1996). This makes the studies look still more different and, in particular, makes Siegmund et al. (1996) appear to be a more extreme outlier relative to the others.

For the studies of Wirth and Egger (1999), Spaete et al. (1994), and Lamarque and Hess (1994), the process studied is in each case a particular synoptic-scale mid-latitude cyclone. Siegmund et al. (1996) applied the Wei method over an entire hemisphere and an entire month. Still, one expects that the largest transport events will involve synoptic-scale systems bearing some resemblance to those in the other studies, and this expectation is supported by the results of the present study. However, the largest value of either  $M_u/M_d$  or (in absolute magnitude)  $M_u/M$  was obtained by Siegmund et al. (1996) from an assimilated dataset, while the others were obtained from free-running model simulations.

Two hypotheses suggest themselves for the difference between the results of Siegmund et al. (1996) and the other three studies (the substantially smaller differences among those other three presumably being explainable by differences in the particular events studied). One is that most of the gross flux occurs in small events, which would be sampled by Siegmund et al. (1996) but not by the others due to their focus on particular individual systems of relatively large amplitude. The other is that the Wei method for some reason yields different results depending on whether the input data come from a free-running model or an assimilated dataset. The results of the present study support both hypotheses to some extent. Much of the gross flux in our calculations does appear to be due to small amplitude events, but a simple order of magnitude calculation (see section 5) suggests that these small events might reasonably be explained as artifacts caused by errors in the input data.

### 3. Implementation

We have implemented the Wei method with the numerical modifications developed by Siegmund et al. (1996). These modifications, referred to by Siegmund et al. (1996) as the “advection method,” are intended to reduce errors associated with the practical problems of time and space differencing. In finite-difference terms, the advection method seeks to rationalize the addition of space and time differentials by selectively averaging the space terms over time. Since the temporal averaging is accomplished along wind vectors, it is “ad-

vective.” Siegmund et al. (1996) fully discuss the mathematics and the reduction of spurious noise that results.

As input data we have used the GEOS assimilation dataset, version 1 (Schubert et al. 1993). These data are available on a  $2^\circ$  latitude by  $2.5^\circ$  longitude by 19 pressure level grid, at 6-hourly time spacing. The vertical resolution is 50 hPa (approximately 1.5 km) around the extratropical tropopause and the uppermost level is 0.4 hPa. We used in this analysis 37 months of data from May 1995 through May 1998, with a focus on January 1996 for comparison with previous work. As a check, we also estimate the net CTF using a mass budget method described by Appenzeller et al. (1996). In contrast to studies that only examine the Northern Hemisphere extratropics in winter, we extend the analysis using the Wei method to the annual cycle over the globe.

The GEOS data have lower spatial and temporal resolution than most of the data used by Siegmund et al. (1996). However, Siegmund et al. (1996) indicate that at smaller time and space scales than those examined here, net fluxes begin to converge. Hoerling et al. (1993) found little quantitative difference between results computed at different horizontal resolutions. The resolution may bring an additional uncertainty into the analysis, though ideally the diagnostic should not be strongly resolution dependent in the range of resolutions typical of available datasets. The basic formulation for the instantaneous CTF per unit horizontal area,  $m$ , in pressure coordinates, is

$$m = \frac{1}{g} \left( -\omega + \mathbf{V}_h \cdot \nabla P_t + \frac{\partial P_t}{\partial t} \right), \quad (5)$$

as introduced by Wei (1987). In (5),  $g$  is the acceleration due to gravity,  $\omega$  is the pressure vertical velocity,  $\mathbf{V}_h$  is the horizontal wind vector, and  $P_t$  is the pressure of the material surface of interest (the tropopause). Wirth and Egger (1999) show how (5) can be derived from (1).

The definition of the material surface for the Wei diagnostic is an important issue. In this case that surface is taken to define the tropopause. Grewe and Dameris (1996) addressed this issue in some detail, using both a thermal definition of the tropopause based on the lapse rate and a dynamic definition of the tropopause based on values of Ertel’s PV. We have chosen to define the tropopause using the dynamic definition, expressed in potential vorticity units (PVU), where  $1 \text{ PVU} = 1 \times 10^{-6} \text{ K kg}^{-1} \text{ m}^2 \text{ s}^{-1}$ . The value of potential vorticity corresponding to the midlatitude tropopause varies from about 1.5 PVU (WMO 1986) to 3.5 PVU (Hoerling et al. 1991). Several analyses (Hoerling et al. 1993, 1991) have shown that 3 or 3.5 PVU is quite close to the thermal tropopause in midlatitudes. The PV value chosen may be related to the resolution of the input data as noted by Hoerling et al. (1993). Higher-resolution analyses (Lamarque and Hess 1994) generally have used lower values of PV. Grewe and Dameris (1996) and Siegmund et al. (1996) have done sensitivity analyses

to PV surface chosen using the Wei diagnostic. To constrain the value of the tropopause surface in the Tropics where PV becomes ill conditioned, we have used a potential temperature surface marking the lower boundary of the stratospheric overworld (Holton et al. 1995) of 380 K.

For exchange of air mass and constituents the tropopause is perhaps best not defined by one surface but by a “region,” for example, bounded by PV surfaces. Fluxes out of this region may be more relevant than those across a single surface. Accordingly, a range of tropopause definitions using different PV surfaces is examined. These tropopause surfaces are described as single valued in the vertical, even in the case of a multiple-valued tropopause in the vertical. When the tropopause “folds” in the vertical, an average tropopause height is used. Some analyses are also run by defining the tropopause as the highest altitude of the selected potential vorticity value [“Assumption A” of Siegmund et al. (1996)]. Both an average and high definition of the tropopause in regions with a multiple-valued tropopause in the vertical yield a few individual points of difference and spatial integrals of the gross and net fluxes that are nearly identical. This may be because, perhaps due to the relatively large grid spacing, there appear to be few major tropopause folding events in the data record used here.

We will also implement the Wei method on a theta surface at the boundary between the lowermost stratosphere and the overworld (Holton et al. 1995), as a link to other work using the downward control principle (Haynes et al. 1991) and residual circulation (Rosenlof 1995; Eluszkiewicz et al. 1996; Gettelman et al. 1997) on surfaces above the tropopause.

## 4. Results

### a. Budget estimate

For comparison to our results obtained using the Wei method, we have calculated the monthly averaged net CTF using GEOS data and the method used by Appenzeller et al. (1996). The net CTF [ $F_{\text{out}}$  in Appenzeller et al. (1996), their Eq. (1)] is defined as the sum of 1) the monthly average change in mass of the lowermost stratosphere and 2) the diabatic mass flux across the upper boundary of the lowermost stratosphere calculated using the diabatic heating rates. The resulting monthly averaged net CTF by hemisphere is illustrated in Fig. 1 for 1996–97. The lowermost stratosphere is defined as the region between the 3-PVU tropopause surface and the 380 K potential temperature surface in the extratropics. The daily and zonally averaged mass flux at the top of this surface is estimated using the daily and zonally averaged diabatic heating and static stability, and the result is then averaged monthly and meridionally from 28° to each pole [the heating rate calculation differs slightly from the method described by Ap-

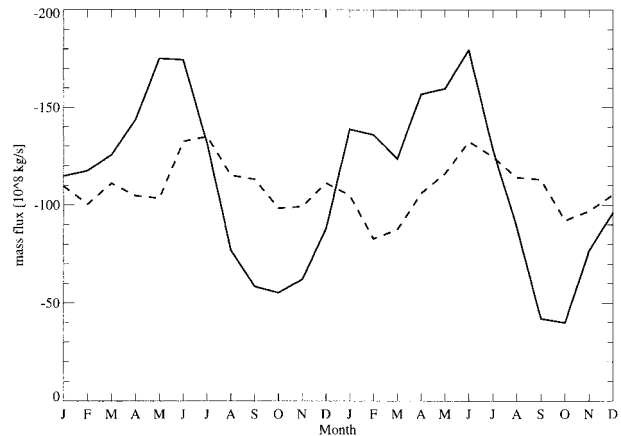


FIG. 1. Monthly averaged net extratropical CTF by hemisphere, calculated from GEOS data, using budget method of Appenzeller et al. (1996). Northern Hemisphere, solid line; Southern Hemisphere, dashed.

penzeller et al. (1996), their Eq. (3), in that they used monthly averaged heating rates from the start rather than performing the monthly average after the mass flux computation]. The result is not very sensitive to the PV value of the tropopause surface or the latitude boundary of the Tropics selected.

The annual cycle timing and amplitude illustrated in Fig. 1 are comparable to those presented by Appenzeller et al. (1996). The Northern Hemisphere mass flux into the troposphere peaks in both winter and spring, a result of the winter peak in the diabatic circulation and the shrinking of the lowermost stratosphere in spring. The difference in net mass flux between hemispheres is also captured. The average Northern Hemisphere net winter mass flux (28°N to pole for December, January, and February) is  $1.2 \times 10^9 \text{ kg s}^{-1}$ , similar to the  $1.4 \times 10^9 \text{ kg s}^{-1}$  found by Appenzeller et al. (1996). Thus, in the extratropics, the GEOS data appear to capture well the long-term budget of mass exchanged between the stratosphere and the troposphere. This provides evidence that any problems that may result when the Wei method is applied to these data cannot be ascribed to the GEOS data's being in any obvious way inferior to other datasets, such as the assimilated data from the U.K. Meteorological Office (UKMO) used by Appenzeller et al. (1996).

### b. Snapshots

Large CTF events may be associated with frontal systems. Figure 2 illustrates the application of the Wei diagnostic for a large-scale frontal system over the eastern seaboard of the United States. The region of large CTF near the tropopause corresponds to a strong gradient in the tropopause height near the winter jet stream marked by strong winds. The large-magnitude CTF at this time is located just west of a surface cold front indicated on surface analyses from the National Centers for Envi-

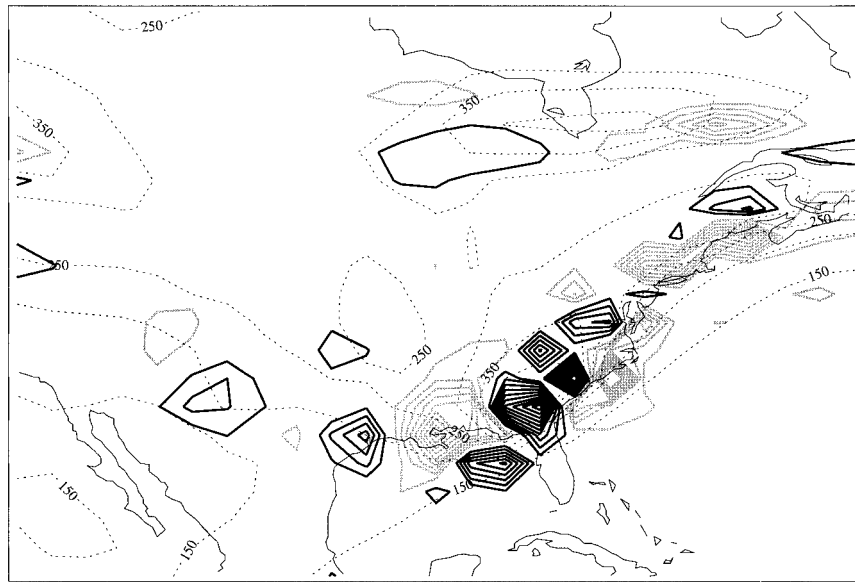


FIG. 2. CTF at 0600 UTC 4 Jan 1996. Solid gray lines are downward instantaneous CTF. Solid black lines, upward CTF. Contour interval of  $1 \times 10^{-2} \text{ kg m}^{-2} \text{ s}^{-1}$ . Dotted lines represent the pressure on the 3-PVU tropopause (in hPa).

ronmental Prediction. There is significant CTF in both directions along the gradient in tropopause height.

A plot of different components of the diagnostic illustrates the situation. High wind speeds and a changing tropopause height are the most important inputs to the calculation, which yield positive and negative values of CTF in rapid succession (Fig. 3a). In general, the winter storm track regions of the Northern and Southern Hemispheres exhibit many of these canonical midlatitude cyclones, with similar features resulting in the Wei diagnostic. There appears in most cases a dipole structure to the CTF, in both time (Fig. 3a) and space (Fig. 3b), with components of tropopause motion and wind relative to the tropopause canceling partially, but not completely. Similar spatial patterns are noted by Siegmund et al. (1996), Lamarque and Hess (1994), and Wirth and Egger (1999). Since this pattern typically persists for a time longer than a characteristic parcel transit time across the dipole structure, the pattern seems to indicate that air travels “through” a region of anomalously low tropopause height, passing from troposphere to stratosphere and then immediately back again. The low tropopause just south of Hudson Bay in Fig. 2 illustrates one case of transport into the stratosphere on the upwind (west) side and out of the stratosphere on the downwind (east) side of a low tropopause feature. A modest mismatch, such as would be caused by an error in the assimilated data, between the analyzed horizontal velocity and the translation speed of the tropopause height anomaly could cause such behavior, though we have no way of telling whether this is the case or whether the diagnosed CTF is correct. Similar problems are noted in the case study described by Wirth and Egger (1999).

In addition to gradients in tropopause height associated with frontal systems, horizontal CTF occurs when tongues of high-PV air are advected to low latitudes and then erode into the troposphere, causing the stratosphere to troposphere exchange of mass. An example of one of these events off the western coast of North America is illustrated in Fig. 4. In this case the structure is subsequently cut off from the stratosphere. This event and the diagnosed pattern of CTF associated with it is similar to many other cut-off cyclone events in the analysis fields. The CTF in Fig. 4 is diagnosed as being into the stratosphere as the tongue approaches and into the troposphere as it passes. The pattern of exchange is coherent and matches the location of the tongue. A similar pattern of exchange first into the stratosphere and then back into the troposphere upstream was noted by Lamarque and Hess (1994). Again, this apparent flow through the tropopause height anomaly could be real, or could be misdiagnosed, or at least exaggerated, by fairly small data errors. One such possible point error in tropopause height is clearly visible in Fig. 4 at  $40^{\circ}\text{N}$  near the east coast of the United States, where a single point anomaly in the tropopause height yields significant gross (but perhaps little net) CTF. These large point errors appear infrequently and randomly in the analyses.

The two structures illustrated in Figs. 2 and 4 appear at first glance to be the dominant forms of extratropical CTF. The distribution in space of the CTF over a month is illustrated in Fig. 5 by averaging the instantaneous CTF over time. The winter hemisphere storm track experiences the greatest variability in CTF in both January (Fig. 5a) and July (Fig. 5b). There is still a high degree of spatial variability, with some regions showing sig-

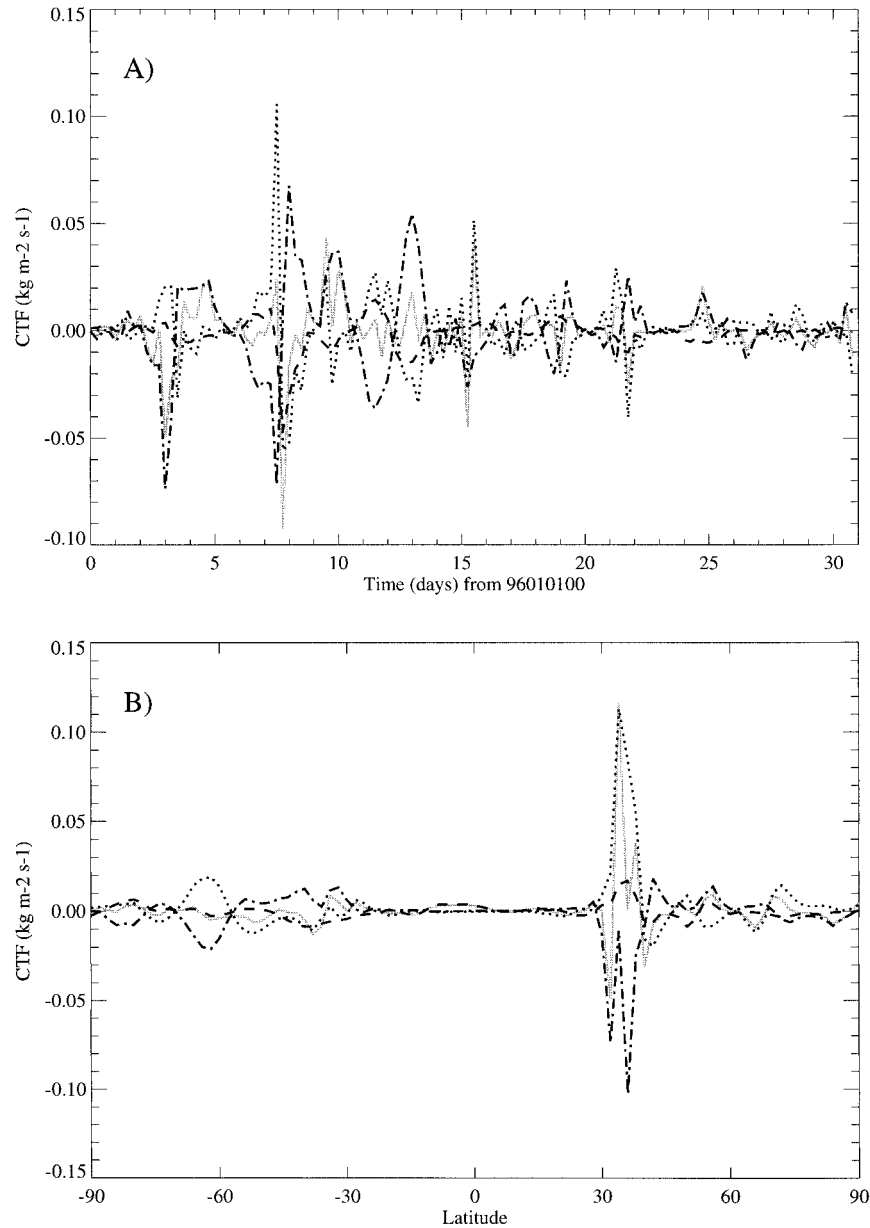


FIG. 3. Components of the Wei diagnostic in units of  $\text{kg m}^{-2} \text{s}^{-1}$ . (a) Time series at  $32^\circ\text{N}$ ,  $80^\circ\text{W}$  for Jan 1996. (b) Latitude section at  $80^\circ\text{W}$  at 0000 UTC 4 Jan 1996. Total CTF gray solid line;  $-\omega$  dashed;  $\mathbf{V} \cdot \nabla P$ , dot-dash;  $\partial P_e / \partial t$  dotted.

nificant average upward fluxes, forming dipoles with adjacent downward average fluxes. The situation for Southern Hemisphere winter is similar to that in the Northern Hemisphere, with structures similar to those in Figs. 2 and 4 but of slightly lower magnitude. Most of the CTF in the Northern Hemisphere winter is confined to distinct portions of the storm track, primarily over the North Pacific east of Japan but also over the eastern United States and North Atlantic. In the Southern Hemisphere winter the largest variability is seen over and around Australia. A strong jet and its asso-

ciated tropopause gradient are the main features of diagnosed CTF.

In neither season is detailed structure in the instantaneous CTF found in the Tropics. Tropical instantaneous CTF is generally positive and of much lower magnitude than in high latitudes. However, there is less cancellation, so that the net mass flux into the stratosphere in the Tropics ends up comparable in magnitude to that out of the stratosphere in the extratropics, as required by mass balance (though the global mass budget, as diagnosed by the Wei method, balances only very

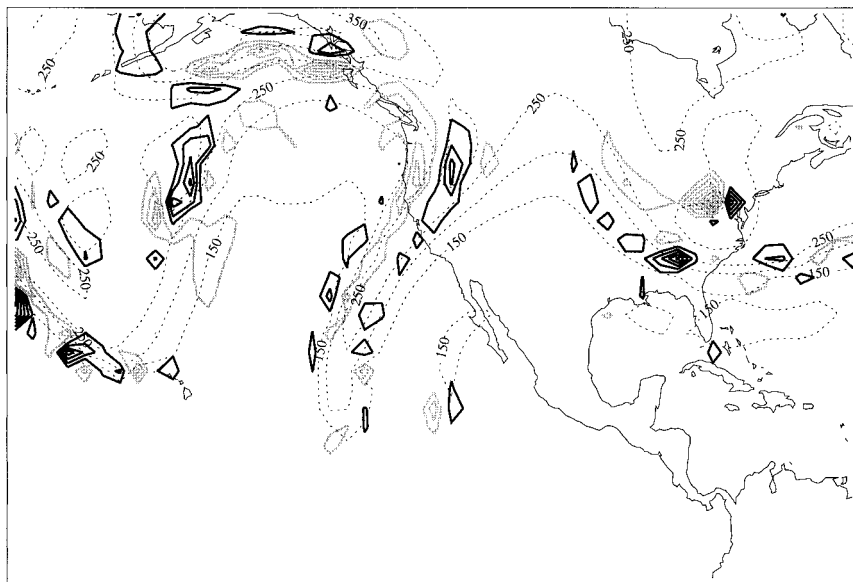


FIG. 4. CTF on 0600 UTC 10 Jan 1996. Solid gray lines are downward instantaneous CTF. Solid black lines, upward CTF. Contour interval of  $1 \times 10^{-2} \text{ kg m}^{-2} \text{ s}^{-1}$ . Dotted lines represent the pressure on the 3-PVU tropopause (in hPa).

roughly, as discussed in section 4d). There appears to be little large-scale organization in the tropical CTF. No patterns directly associated with the monsoon circulations are visible. It is reasonable to expect that the tropical results are more strongly affected by weaker aspects of the assimilation system, such as the convection scheme in the model used for the assimilation, than are the extratropical results. For this reason we limit our attention to the extratropical results hereafter.

In midlatitudes, summertime frontal systems, which generate summertime convection, do seem to have significant tropopause gradients associated with them and generate CTF structures similar to those noted in the winter season. However, nonfrontal convective activity does not appear to generate any such structures. Convective activity over Florida in June 1996, for example, appears on several days over regions larger than the size of a grid box in the GEOS assimilation for periods longer than 6 h according to NEXRAD radar analyses, without any evidence of significant CTF. This result is subject to the same caveat as the tropical results; that is, it may be relatively sensitive to the diabatic parameterizations in the model.

In summary, analysis of the instantaneous CTF reveals that the midlatitude storm track regions have the highest instantaneous and temporally averaged values of CTF and that midlatitude synoptic-scale systems and horizontal tongues of tropopause air are responsible for much of this gross exchange. Exchange from the troposphere into the stratosphere is found to occur in many of these events, though much of this is immediately compensated by exchange from the stratosphere back into the troposphere, suggesting flow “through” tro-

popause height anomalies rather than irreversible exchange. This phenomenon could possibly be explained by relatively small errors in the input data (as will be discussed further below), and hence its veracity may be questioned. Tropical instantaneous CTF is marked by low-magnitude upward drift and does not have significant regional structure.

### c. Monthly and seasonally integrated results

The monthly and seasonally integrated CTF are presented in this section. We integrate the instantaneous CTF over time and area to generate the net flux ( $M$ ) for comparison with other methods of quantifying stratosphere–troposphere exchange. Several approaches to integrating the instantaneous cross-tropopause flux in space and time will be explored. The method is also extended to look at isentropic surfaces. Globally and annually integrated results are presented in section 4d.

Many of the previous analyses of stratosphere–troposphere exchange with the Wei method and others have focused on the extratropics of the Northern Hemisphere in winter. Accordingly, integrating the instantaneous CTF for comparison and averaging for December, January, and February (DJF) of 1996 yields an average downward flux from  $28^\circ$  to  $90^\circ\text{N}$  of  $387 \times 10^8 \text{ kg s}^{-1}$  ( $1 \times 10^{17} \text{ kg month}^{-1}$ ) for a 3-PVU tropopause. The corresponding values for DJF 1996–97 and 1997–98 are  $404 \times 10^8$  and  $280 \times 10^8 \text{ kg s}^{-1}$ , respectively (see section 4d). For January 1996, the average CTF with an extratropical tropopause defined by different PV surfaces is  $334 \times 10^8$ ,  $314 \times 10^8$ , and  $277 \times 10^8 \text{ kg s}^{-1}$  for the 2-, 3-, and 5-PVU surfaces, respectively, with a

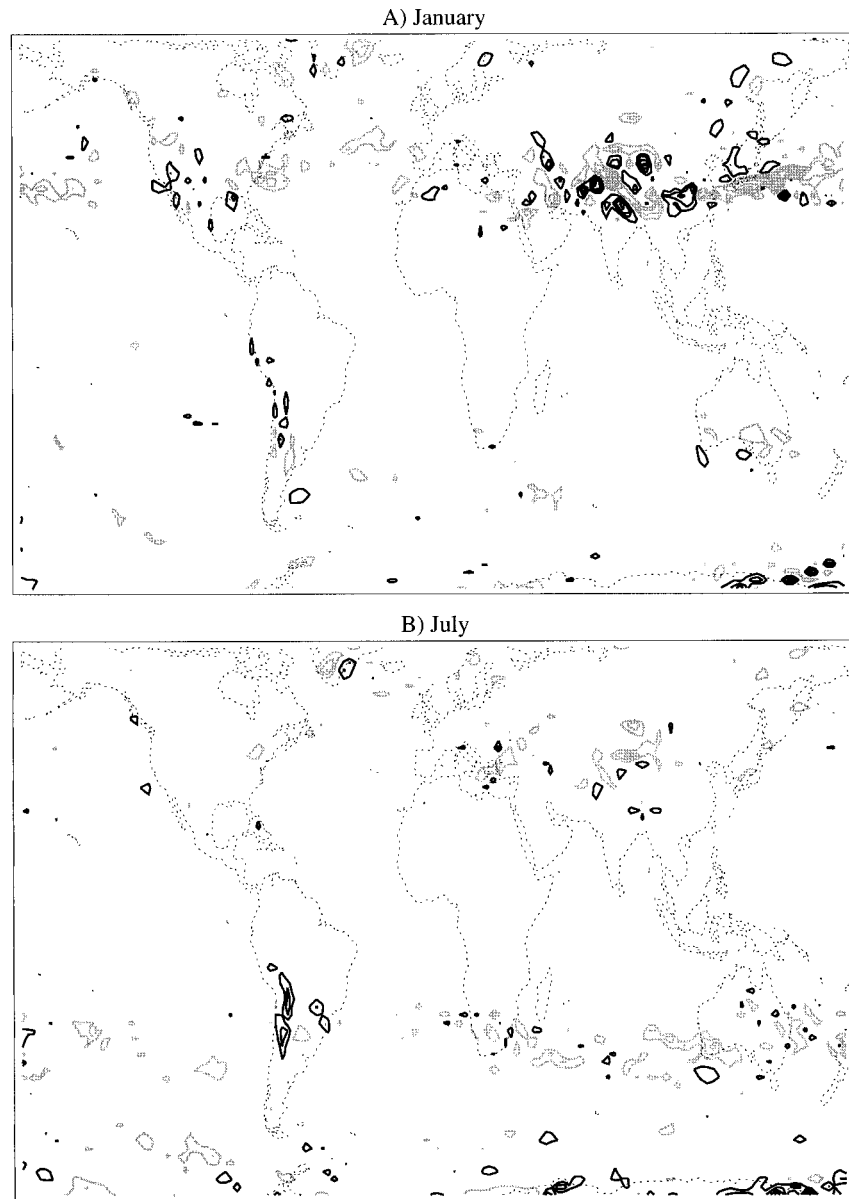


FIG. 5. Monthly averaged CTF for (a) Jan and (b) Jul. Black lines are average upward CTF, gray lines are downward CTF. Contour interval  $2 \times 10^{-3} \text{ kg m}^{-2} \text{ s}^{-1}$ .

gradient of about  $20 \times 10^8 \text{ kg s}^{-1}$  per PVU ( $5 \times 10^{15} \text{ kg month}^{-1}$ ). These fluxes are presented graphically in Figs. 6a and 6b. The gross upward and downward fluxes ( $M_u$  and  $M_d$ ) over a month for January are  $10.7 \times 10^{17} \text{ kg up}$  and  $11.6 \times 10^{17} \text{ kg down}$ , and the ratio  $M_u/M_d = 0.92$ , consistent with Siegmund et al. (1996). In addition, the probability density function of instantaneous CTF over a month is virtually identical to that of Siegmund et al. (1996).

The net fluxes indicated in Fig. 6 are highly dependent upon the latitude chosen to define the equatorward boundary of the extratropics. Figure 7 illustrates the integrated monthly flux by latitude for these various

surfaces. The latitude  $28^\circ\text{N}$  is taken to represent the approximate point at which the zonally averaged integrated flux becomes positive as latitude decreases toward the equator. As found by Hoerling et al. (1993) and Siegmund et al. (1996), there are latitudes in which there is net upward CTF in the extratropics over the course of a month. The upward flux arises due to the dipole structures illustrated in the average monthly flux as shown in Fig. 5a. These are present because the instantaneous dipole structures, as in Fig. 3a, tend to recur in the same locations and are quasi-zonally oriented so that they do not disappear in a zonal and time average. Similar patterns have been seen in vertically

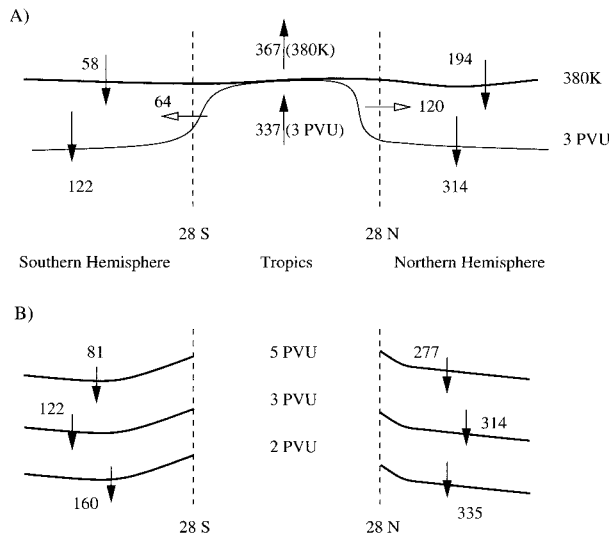


FIG. 6. Budget calculations for Jan 1996 monthly integrated net CTF in units of  $10^8 \text{ kg s}^{-1}$  in the bounded regions for (a) tropopause and 380 K theta surface in the extratropics and (b) different PV definitions of the extratropical tropopause.

folded tropopause events by Lamarque and Hess (1994).

In principle, the Wei method can be used to describe transport across any material surface in the atmosphere. While PV and potential temperature surfaces have been used here and in previous studies to define the tropopause, it is also useful in discussing stratosphere–troposphere exchange to look at exchange with the stratospheric overworld (Holton et al. 1995), that is, exchange across the 380K potential temperature surface. The advection method has been applied to analyses of potential temperature at this and other levels as a way of diagnosing this exchange near 100 hPa. The net extratropical downward flux from 28° to 90°N for January 1996 at 380 K is  $194 \times 10^8 \text{ kg s}^{-1}$ , as illustrated in Fig. 6. The flux by latitude across the 380 K surface is also plotted in Fig. 7. Note that at 380 K there is no upward flux in the extratropics.

The flux across 380 K, along with the flux at the tropopause, implies a quasi-isentropic flux in the middle-world from the Tropics (at 28°N) of  $120 \times 10^8 \text{ kg s}^{-1}$ , as illustrated in Fig. 6b. In the Southern Hemisphere the circulation is less vigorous, with a net transport of  $58 \times 10^8 \text{ kg s}^{-1}$  downward across the 380 K surface and  $122 \times 10^8 \text{ kg s}^{-1}$  downward at the tropopause (3 PVU), implying a net influx from the Tropics of  $64 \times 10^8 \text{ kg s}^{-1}$  at 28°S. However, the tropical fluxes do not balance this influx. Tropical fluxes imply more air rising above 380 K than crossing the tropopause in the Tropics, which would imply net quasi-isentropic fluxes of the opposite sign to those shown in Fig. 6b. The maximum gross fluxes at 380 K are an order of magnitude lower than those at the tropopause, while typical gross fluxes are a factor of 2 lower than at the tropopause. This may

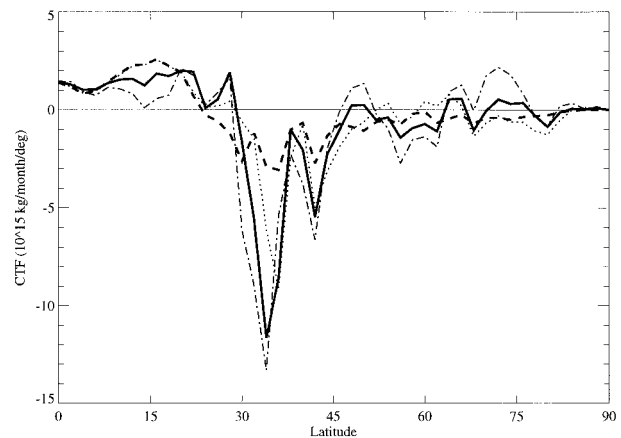


FIG. 7. Zonally averaged monthly extratropical CTF for the Northern Hemisphere, by latitude, units of  $10^{15} \text{ kg month}^{-1} \text{ degree}^{-1}$ . 2-PVU tropopause: dot-dash; 3-PVU tropopause: solid; 5-PVU tropopause: dotted; 380 K surface: dashed.

be due to the reduction of synoptic-scale activity with height above the tropopause. However, the net flux is still of the same order of magnitude because as for the tropopause, the smaller events dominate the net flux (see section 5). These fluxes are not directly comparable to fluxes across the 100-hPa pressure surface, because the surfaces are not coincident. Especially in the Northern Hemisphere in winter, the 380 K surface is significantly below the 100-hPa surface.

To compare the magnitude of the extratropical flux integrated over a month with other studies, one must be careful to apply the definition of “extratropics” consistently. Different studies use different definitions. These studies also examine different years, so that interannual variability may cause some variation in the results. The quantitative results presented above translate into a net downward CTF for January 1996 of  $64 \times 10^{15} \text{ kg}$  for 14°–90°N,  $80 \times 10^{15} \text{ kg}$  for 24°–90°N, and  $84 \times 10^{15} \text{ kg}$  for 28°–90°N. The values reported here are within the range of previous estimates. Figure 8 puts the results here (filled points) in the context of other estimates of the Northern Hemisphere extratropical mass flux averaged over December, January, and February (DJF) at various levels. Note the vertical axis is by approximate vertical level and the horizontal axis is logarithmic. Different studies are as indicated in the caption, and the different shapes indicate different methods. Ranges are indicated where known. Generally, there is an increase in the reported exchange of mass between the stratosphere and troposphere with decreasing altitude. CTF estimated using the Wei method is generally a factor of 2 larger than most estimates of stratosphere–troposphere exchange of air calculated using budget methods [Appenzeller et al. (1996) and this study] or estimated using the residual circulation in the stratosphere (Rosenlof 1995; Gettelman et al. 1997; Yang and Tung 1996). The magnitude of the discrepancy appears to be consistent throughout the year (see section

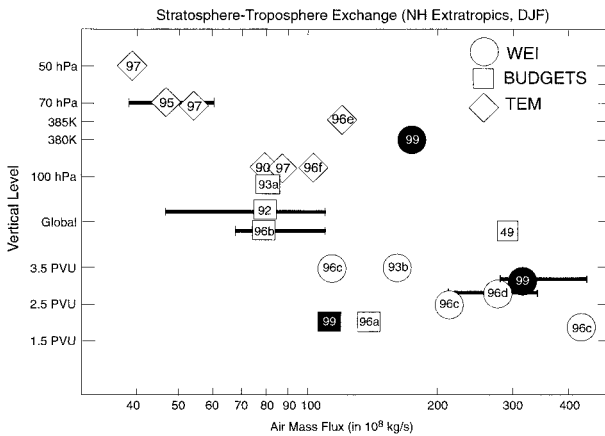


FIG. 8. Average Dec, Jan, and Feb extratropical CTF for the Northern Hemisphere in units of  $10^8 \text{ kg s}^{-1}$ . Symbols represent different methods as discussed in the text. Values in this study in black. Studies cited by year of publication as follows: Brewer, (1949; 49), Holton (1990; 90), Follows (1992; 92), Rosenlof and Holton (1993; 93a), Hoerling et al. (1993; 93b), Rosenlof (1995; 95), Appenzeller et al. (1996; 96a), van Velthoven and Kelder (1996; 96b), Siegmund et al. (1996; 96c), Grewe and Dameris (1996; 96d), Yang and Tung (1996; 96e), Eluszkiewicz et al. (1996; 96f), and Gettelman et al. (1997; 97).

4d). The Wei method appears to yield results that are larger than those derived by other methods, even at higher altitudes (such as the 380 K potential temperature surface). Wei method calculations at the tropopause level here are within the range of other studies. Note that the CTF estimate of  $1.2 \times 10^9 \text{ kg s}^{-1}$  using GEOS data and the mass budget approach of Appenzeller et al. (1996), as discussed in section 4a, is significantly lower than the estimate obtained from the Wei method using the same data but comparable to the estimate of Appenzeller et al. (1996).

#### d. Globally and annually integrated results

In this section we present the mass flux across the tropopause using the Wei method integrated over the entire globe and over a whole year. We then compare this result to an integration of the mass flux across a coincident pressure surface for an entire year. In principle both calculations should give a number comparable to the annual change in mass of the stratosphere. Figure 9 first illustrates the annual cycle of CTF integrated from  $28^\circ$  to  $90^\circ\text{N}$  for three years from May 1995 through May 1998. The largest downward flux in the Northern Hemisphere midlatitudes generally occurs in January and February, with the minimum in August. The annual cycle of the diagnostic is consistent with the cycle of the residual circulation at 100 hPa (Rosenlof 1995; Gettelman et al. 1997), lagging it by a month or two. The lag in CTF is less than that estimated in section 4a, using heating rates and the mass of the lowermost stratosphere. The magnitude of the net extratropical CTF from  $28^\circ$  to  $90^\circ\text{N}$  throughout the year is about twice

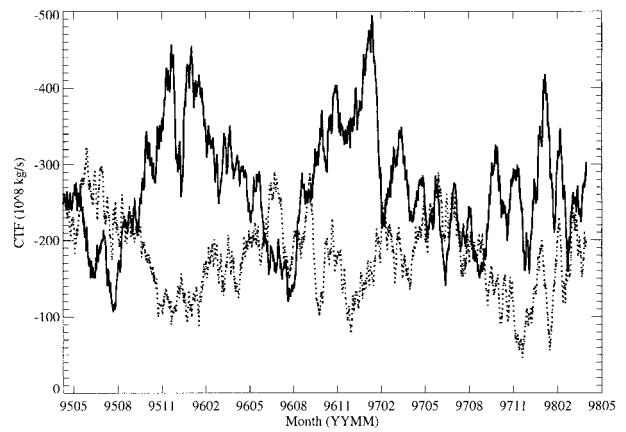


FIG. 9. Monthly averaged extratropical CTF from  $28^\circ$  to  $90^\circ\text{N}$  for the Northern (solid) and Southern (dashed) Hemispheres, in units of  $10^8 \text{ kg s}^{-1}$ . Data have been smoothed with a 21-day running mean filter.

the magnitude found in section 4a and by Appenzeller et al. (1996). The annual cycle of net CTF in the Southern Hemisphere extratropics has a smaller amplitude and has a broad peak in July. The difference in CTF between hemispheres is larger than that previously noted by Appenzeller et al. (1996). There are significant interannual differences between years noted in Fig. 9, particularly in the Northern Hemisphere winter CTF. The peak flux varies by nearly 25% from year to year, and the average over the winter (DJF) varies from  $280 \times 10^8 \text{ kg s}^{-1}$  in 1997–98 to  $404 \times 10^8 \text{ kg s}^{-1}$  in 1996–97. The causes for this variability have not been explored in detail.

The atmospheric mass above the tropopause or the 380 K surface changes by a relatively small fraction over the course of a year. Hence if the computed net flux across a surface is a much larger fraction of the total mass above the surface, we know there is an error in the calculation whose magnitude is of the order of the discrepancy. This provides a strong check on the accuracy of the calculations, which has not been done in previous studies using the Wei method.

A global integral of the mass flux over an entire year from August 1995 to August 1996 yields a residual of  $-3 \times 10^{17} \text{ kg}$  (which averages to  $-95 \times 10^8 \text{ kg s}^{-1}$ ) at the tropopause and  $+4 \times 10^{17} \text{ kg}$  (an average of  $+125 \times 10^8 \text{ kg s}^{-1}$ ) at 380 K. With the mass of the stratosphere on the order of  $11 \times 10^{17} \text{ kg}$  (Appenzeller et al. 1996), these fluxes are quite large. Integrating the mass flux across a pressure surface (which is simply the pressure vertical velocity,  $\omega$ , divided by the acceleration due to gravity,  $g$ ; the Wei method per se need not be used for this calculation) near the tropopause (300 hPa) or near the 380 K surface (100 hPa) yields residuals that are an order of magnitude smaller and of the same order as potential mass changes of the stratosphere over the course of a year, that is, a few percent or less (Appenzeller et al. 1996). Thus the errors are not caused by biases in the assimilated vertical velocities. The more

likely explanation appears to be errors in the diagnoses of the PV and horizontal velocity normal to the tropopause, the same source of errors noted by Wirth and Egger (1999). The next section illustrates how what may appear to be a relatively small amount of noise or bias in the PV or potential temperature fields can yield relatively large errors in the CTF diagnosed by the Wei method.

### 5. Effect of input data errors

Consider the tropopause to be explicitly represented as a PV surface, and choose the sign of  $\hat{\mathbf{n}}$  so that

$$\hat{\mathbf{n}} = -\frac{\nabla Q}{|\nabla Q|},$$

where  $Q$  is the PV. We now consider the true PV,  $Q$ , to be represented by an assimilated dataset subject to errors, so that the analyzed PV is

$$Q_a = Q + e.$$

Clearly  $e$  should include observation errors. We argue below that it should also include the ‘‘nudging’’ terms in an assimilated dataset.

The normal component of the analyzed PV surface velocity can then be written as

$$\mathbf{u}_c \cdot \hat{\mathbf{n}} = \frac{\partial Q_a}{\partial t} (\nabla Q_a)^{-1} = \left( \frac{\partial Q}{\partial t} + \frac{\partial e}{\partial t} \right) (\nabla Q_a)^{-1}. \quad (6)$$

The evolution equation for the true PV is

$$\frac{\partial Q}{\partial t} = -\mathbf{u} \cdot \nabla Q + S, \quad (7)$$

where  $S$  represents true physical sources and sinks of PV due to heating, friction, and subgrid-scale effects. Using (7) and (6) with (1) leads to

$$\tilde{m} = \left( S + \frac{\partial e}{\partial t} \right) (\nabla Q_a)^{-1}, \quad (8)$$

where we have neglected the difference between  $\nabla Q$  and  $\nabla Q_a$  in the advective term in (7).

Equation (8) shows that the sensitivity of Wei’s method to input data errors depends on the relative magnitudes of the true nonconservative sources and sinks of PV and on the spurious apparent source due to errors. In an assimilated dataset,  $\partial e/\partial t$  should include the nudging terms that force the model PV back toward observations. These terms are necessary because of inconsistencies between the PV tendencies predicted by the dynamical model used in the assimilation and the observed PV tendencies. These inconsistencies may result from observational errors, errors in the simulated PV advection, or errors in the simulated nonconservative PV sources and sinks. Therefore, the magnitude of the nudging terms must be considered representative of the magnitude of the uncertainty in both the advection and

the nonconservative terms, which collectively are represented by  $\partial e/\partial t$  in (8).

The approximate conservation of PV, which is commonly assumed in discussions of midlatitude dynamics, implies that  $S \ll |\mathbf{u} \cdot \nabla Q|$ . This means that the error term can be small compared to the advective term in the evolution of the analyzed PV, so that the analyzed data can ‘‘look good’’ in the sense of exhibiting the expected tracerlike spatial and temporal structure in the PV field, while simultaneously  $S \leq \partial e/\partial t$ , so that the error term is significant or even dominant in mass flux calculations using the Wei method, and therefore the signal to noise ratio in the instantaneous CTF is of order unity or less. Sobel et al. (1997) discussed a similar problem with the trajectory-based ‘‘contour crossing’’ method, which has been used to diagnose transport across the edge of the stratospheric polar vortex.

In short, the Wei method places a very strict demand on an observed or assimilated dataset by requiring that errors in the simulated PV tendency be small compared to the actual nonconservative terms, which in turn are generally small compared to advection. It is not clear that any currently available observed or assimilated dataset meets this requirement.

To make the point more quantitative, consider the results of this analysis, for the Northern Hemisphere extratropics (28°–90°N) in January. A typical value obtained for the instantaneous CTF is of order  $\sim 10^{-2}$  kg m<sup>-2</sup> s<sup>-1</sup> or less. Assuming a typical midlatitude tropopause value for the air density of 0.3 kg m<sup>-3</sup>, this corresponds to  $|\mathbf{u} - \mathbf{u}_c| \sim 0.03$  m s<sup>-1</sup>. With 6-hourly data this velocity corresponds to a displacement over 6 h of about 600 m, which at tropopause altitudes is less than the vertical grid spacing of the input dataset. Hence spurious ‘‘jitter’’ in the analyzed tropopause height tendency need not even be a single vertical grid spacing per 6 h for the results to be attributed to input data errors at the 100% level, as far as the instantaneous CTF is concerned. The same conclusion holds for the results of Siegmund et al. (1996), if the appropriate values from their study are inserted in the rough calculation above.

It might be plausible to suppose that when the instantaneous CTF is heavily integrated over space and time to produce a net mass flux  $M$ , the effect of the analysis errors ought to largely cancel out. However, given the lack of mass balance over the course of a year, as seen in section 4d, it appears that this is not entirely the case. This mass imbalance suggests that the errors in the assimilated data have a persistent bias. In the case of a potential temperature surface (such as 380 K), this could be caused by a persistent cold or warm bias in the model, which would lead to a spurious net heating or cooling as the model was nudged toward observations. The bias would not need to be present in the vertical integral, but only at the level of the surface in question. For a PV surface, a persistent bias in the model’s potential temperature gradient could cause a systematic bias in the diagnosed CTF.

In any case, spatial and temporal averaging removes much of the information relevant to two-way property fluxes ( $M_u$  or  $M_d$ ), which is a significant disadvantage since the potential (in principle) of the Wei method to provide this information is its main advantage over other methods. One may imagine that the error-induced component of the instantaneous flux might have short spatial and temporal timescales, as discussed to some extent by Siegmund et al. (1996), so that one could perform some sort of limited, local averaging to remove the spurious component while leaving some true, physical component behind; in fact, the results quoted for Siegmund et al. (1996) and the results reported in this study already contain a limited amount of spatial averaging using the advection method. The difficulty with such averaging is that there may be true, physical transport mechanisms with comparably short spatial and temporal scales, which would also be averaged out in the process. Too little is known about the real mechanisms of stratosphere–troposphere exchange to judge how great this difficulty is or what spatial or temporal averaging scales might be optimal.

Another way of dealing with input data errors in the diagnostic analysis is to separate large-amplitude structured CTF events (as in the snapshots described earlier), from small-amplitude events, which could be defined as noise. A threshold value might be used to separate the small-amplitude events from large-amplitude ones. Such an analysis has been applied to the instantaneous CTF over the entire globe, and the results have been integrated over a month to obtain the net and gross mass fluxes including only instantaneous fluxes larger than a given threshold in the integrating process. The  $M_u$  and  $M_d$  are sensitive to the threshold value chosen. The two-way fluxes drop rapidly in absolute magnitude for higher threshold values, illustrated in Fig. 10a. As less of the instantaneous CTF is above the threshold, the net flux ( $M$ ) initially increases, then begins to decrease (Fig. 10b). If we were to make the ad hoc assumption that the two-way fluxes ought to be both small in absolute magnitude and independent of the threshold chosen, this analysis would then imply that the optimum threshold value is approximately  $2 \times 10^{-2} \text{ kg m}^{-2} \text{ s}^{-1}$ , since this value does not change the net flux but reduces  $M_u$  and  $M_d$  substantially.

This definition of noise could, however, be missing real systematic transport that simply occurs at low amplitude. Separating “major” events from “minor” events using a threshold value of  $2 \times 10^{-2} \text{ kg m}^{-2} \text{ s}^{-1}$  indicates that  $\frac{2}{3}$  of the upward and downward gross fluxes occur in minor events, and only  $\frac{1}{3}$  in major events. The minor events have a fairly constant magnitude over the period of a month, with a constant level of variability. However, since the minor events are fairly evenly distributed, the total net mass flux does not change proportionately. An appropriate choice of threshold value can thus significantly change  $M_u$  and  $M_d$  without changing the net mass flux. It is unclear

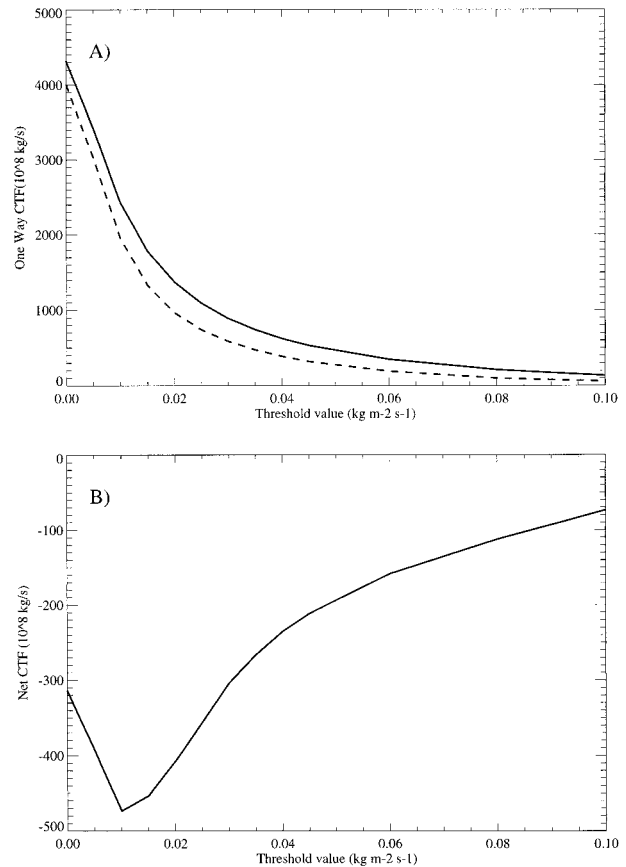


FIG. 10. The effect of changing threshold value on (a) the gross upward ( $M_u$  dashed) and downward ( $M_d$  solid) CTF and (b) the net average CTF for the Northern Hemisphere extratropics ( $28^\circ$ – $90^\circ$ N). CTF units of  $10^8 \text{ kg s}^{-1}$ . Horizontal axis illustrates the threshold value in absolute magnitude below which events are treated as noise. CTF from Jan 1996.

whether the choice of threshold value can be given a physical basis, though the curves in Fig. 10 do have the same shape and approximately the same relationship to the threshold value in Northern Hemisphere summer (July) as in the curves shown for Northern Hemisphere winter (January), except that the flux more rapidly approaches zero as the threshold value becomes high.

## 6. Conclusions

The diagnostic formulation developed previously by Wei (1987) and other authors has been applied to examine mass fluxes across various surfaces near the tropopause. The GEOS assimilated dataset has also been shown to yield net stratosphere–troposphere exchange estimates comparable to those obtained by Appenzeller et al. (1996) with UKMO data, using essentially the same hemispheric mass budget method used by those authors. The instantaneous results of the Wei method implemented with the GEOS data imply that the flux of mass across a tropopause surface (CTF) is an episodic

process. The largest values of CTF are found in winter in midlatitudes, associated with synoptic-scale midlatitude cyclones and related processes. The diagnostic also indicates CTF associated with synoptic and mesoscale activity in the summer season at midlatitudes. Midlatitude CTF at the spatial and temporal resolution of this analysis appears to have a strong dipole structure of positive and negative exchange, especially when strong tropopause gradients are advected by the wind fields. This result is robust, and has been noted by previous authors (Lamarque and Hess 1994) in more detailed studies of individual events. Varying the definition of the tropopause between an average height and a maximum height for a multiple-valued tropopause did not significantly alter the integrated or instantaneous fluxes in this analysis, possibly because few examples of a vertically folded tropopause were found in this analysis due to the low resolution of the assimilation dataset.

In the Tropics, slow uplifting processes are evident in the diagnosed instantaneous CTF, which is of much lower magnitude than in the midlatitudes. Tropical instantaneous CTF does not exhibit significant large-scale organization and is nearly uniform throughout the Tropics. Two possible conclusions might be inferred from this result. If the diagnostic is correct in diagnosing the magnitude of CTF in the Tropics, then the method indicates that tropical CTF is dominated by slow and relatively steady diabatic motion such as that described by Wirth (1996), and the organization of convection in the Tropics does not locally contribute to the flux of air across the tropopause. Alternatively, it may be concluded that perturbations associated with convection may not be diagnosed correctly.

The quantitative results presented here for Northern Hemisphere extratropical wintertime CTF averaged over a month agree with previous estimates using this method but are generally larger than comparable estimates using other methods (Fig. 8). Some studies (Siegmund et al. 1996) reported lower quantitative estimates of the net extratropical wintertime CTF with increasing resolution, though other studies (Hoerling et al. 1993) have found no change in magnitude of the net CTF with resolution. The annual cycle of net extratropical downward fluxes predicted by the diagnostic does appear to match other estimates of stratosphere–troposphere exchange qualitatively, with a maximum in Northern Hemisphere winter. The average magnitude of the net CTF is larger in the Northern than Southern Hemisphere extratropics. The annual cycle amplitude is also stronger in the Northern than Southern Hemisphere extratropics. There is significant short-term variability of the net extratropical flux, which appears on top of the annual cycle, and significant year to year variability. While the annual cycle appears qualitatively reasonable, the magnitude of the CTF appears consistently large over the course of a year. Globally and annually integrated mass budgets have large errors, on the order of 30%–40% of the mass of the stratosphere, which are probably due to persistent

biases in the input data. Because global, annual integrals of pressure vertical velocity on pressure surfaces show much lower residuals, it appears that the errors in this heavily integrated budget are in large part due to persistent biases in the potential vorticity and/or horizontal wind fields (vertical velocity errors must surely contribute to gross fluxes, however, and hence to  $M_u$  and  $M_d$ ). It should be emphasized that the Wei method is particularly sensitive to such input data errors, as also shown by Wirth and Egger (1999), so that the errors need not be large by other standards in order for the problems discussed here to become significant. This conclusion is supported by the quite different and presumably more nearly correct result obtained for the net CTF calculated using a budget method (which *assumes* a balanced mass budget) in section 4a, compared to that obtained from the Wei method.

The net CTF, even for individual synoptic events, is a residual of large upward and downward fluxes. We have argued that these are probably exaggerated by the effect of errors in the input data—even if those errors are not large—and hence that the gross fluxes ( $M_u$  and  $M_d$ ) computed when no threshold is used are probably unrealistically large in magnitude, implying similarly exaggerated tracer fluxes. This exaggeration is reduced by applying a threshold, but there is no physical basis (at least at present) for choosing the threshold value. Hence it may be more desirable to estimate tracer fluxes by other means. For long-lived constituents, which behave as conserved tracers in the region of the tropopause and which have large gradients across it (such as ozone), mass budget analyses (setting  $M_u = 0$  at some surface well above the tropopause) are sufficient to determine the stratosphere–troposphere tracer flux, as shown by Gettelman et al. (1997) and Tie and Hess (1997). However, for shorter-lived species, such as nitrogen oxides, such calculations require that chemistry and two-way transport be considered explicitly. Therefore, in addition to the net mass flux  $M$ , even under strong simplifying assumptions, another piece of information is required, such as  $M_u$ . In principle, the Wei method might provide useful information about these species, by enabling us to compute  $M_u$  and  $M_d$ , but its high sensitivity to relatively small errors in the input data mitigates the usefulness of this approach.

In short, the Wei method may be a useful tool for studying some aspects of stratosphere–troposphere exchange, but it should not be used as a black box. In the absence of a better mechanistic understanding of non-conservative processes occurring around the tropopause than we currently have, quantitative information obtained from this method as applied to current assimilated datasets should be interpreted with caution. Our analysis by itself suggests that the method should provide somewhat more reliable quantitative results when applied to pure model simulations—as in Lamarque and Hess (1994) and Spaete et al. (1994)—though even in that case, Wirth and Egger (1999) find difficulties similar to

those discussed here. Additionally, even if the noise problem is absent or ignored, it is still not entirely clear how much of the CTF represents true irreversible stratosphere–troposphere exchange and how much may represent short-term excursions of air parcels across the tropopause and back with little attendant mixing, but this could perhaps be studied by other methods in conjunction with the Wei method. For purposes of diagnosing the cross-tropopause fluxes of long-lived trace constituents on a global or hemispheric basis, other methods are probably more trustworthy at present.

*Acknowledgments.* We would like to thank three anonymous reviewers for their comments on this manuscript, which led to a number of improvements. We would also like to thank V. Wirth and J. Egger for providing us with a preprint of their paper, performed independently, while the present paper was at the revision stage, so that their paper could be referenced here. Thanks are due to J. A. Kettleborough for some key insights and help with the finite differencing in this work, and to J. R. Holton for discussions and encouragement. AG is supported by a NASA Graduate Student Research Program Fellowship. AHS is supported by the NOAA Postdoctoral Program in Climate and Global Change, administered by the University Corporation for Atmospheric Research's Visiting Scientist Program. Computer resources were provided through the Atmospheric Chemistry Modeling and Analysis Program at Goddard Space Flight Center (A. Douglass, PI) and at UW through NASA Grant NAG-1-1083.

## REFERENCES

- Appenzeller, C., J. R. Holton, and K. H. Rosenlof, 1996: Seasonal variation of mass transport across the tropopause. *J. Geophys. Res.*, **101** (D10), 15 071–15 078.
- Brewer, A. W., 1949: Evidence for a world circulation provided by the measurements of helium and water vapor distribution in the stratosphere. *Quart. J. Roy. Meteor. Soc.*, **75**, 351–363.
- Eluszkiewicz, J., and Coauthors, 1996: Residual circulation in the stratosphere and lower mesosphere as diagnosed from Microwave Limb Sounder data. *J. Atmos. Sci.*, **53**, 217–240.
- Follows, M. J., 1992: On the cross-tropopause exchange of air. *J. Atmos. Sci.*, **49**, 879–882.
- Gottelman, A., J. R. Holton, and K. H. Rosenlof, 1997: Mass fluxes of O<sub>3</sub>, CH<sub>4</sub>, N<sub>2</sub>O and CF<sub>2</sub>Cl<sub>2</sub> in the lower stratosphere calculated from observational data. *J. Geophys. Res.*, **102** (D15), 19 149–19 159.
- Grewe, V., and M. Dameris, 1996: Calculating the global mass exchange between the stratosphere and troposphere. *Ann. Geophys.*, **14**, 431–442.
- Haynes, P. H., C. J. Marks, M. E. McIntyre, T. G. Shepherd, and K. P. Shine, 1991: On the “downward control” of extratropical diabatic circulations by eddy-induced mean zonal forces. *J. Atmos. Sci.*, **48**, 651–679.
- Hoerling, M. P., T. K. Schaack, and A. J. Lenzen, 1991: Global objective tropopause analysis. *Mon. Wea. Rev.*, **119**, 1816–1831.
- , —, and —, 1993: A global analysis of stratospheric–tropospheric exchange during northern winter. *Mon. Wea. Rev.*, **121**, 162–172.
- Holton, J. R., 1990: On the global exchange of mass between the stratosphere and troposphere. *J. Atmos. Sci.*, **47**, 392–395.
- , P. H. Haynes, A. R. Douglass, R. B. Rood, and L. Pfister, 1995: Stratosphere–troposphere exchange. *Rev. Geophys.*, **33** (4), 403–439.
- Hoskins, B. J., 1991: Towards a PV- $\theta$  view of the general circulation. *Tellus*, **43A**, 27–35.
- Lamarque, J.-F., and P. G. Hess, 1994: Cross-tropopause mass exchange and potential vorticity budget in a simulated tropopause folding. *J. Atmos. Sci.*, **51**, 2246–2269.
- Lelieveld, J., and P. J. Crutzen, 1994: Role of deep cloud convection in the ozone budget of the troposphere. *Science*, **264**, 1759–1761.
- Rosenlof, K. H., 1995: Seasonal cycle of the residual mean meridional circulation in the stratosphere. *J. Geophys. Res.*, **100** (D3), 5173–5191.
- , and J. R. Holton, 1993: Estimates of the stratospheric residual circulation using the downward control principle. *J. Geophys. Res.*, **98**, 10 465–10 479.
- Schubert, S. D., R. B. Rood, and J. Pfaendner, 1993: An assimilated dataset for earth science applications. *Bull. Amer. Meteor. Soc.*, **74**, 2331–2342.
- Shaw, W. N., 1930: *Manual of Meteorology*. Vol III, *The Physical Processes of Weather*, Cambridge University Press, 445 pp.
- Siegmund, P. C., P. F. J. van Velthoven, and H. Kelder, 1996: Cross-tropopause transport in the extratropical northern winter hemisphere, diagnosed from high-resolution ECMWF data. *Quart. J. Roy. Meteor. Soc.*, **122**, 1921–1941.
- Sobel, A. H., R. A. Plumb, and D. W. Waugh, 1997: Methods of calculating transport across the polar vortex edge. *J. Atmos. Sci.*, **54**, 2241–2260.
- Spaete, P., D. R. Johnson, and T. K. Schaack, 1994: Stratospheric–tropospheric mass exchange during the Presidents’ Day storm. *Mon. Wea. Rev.*, **122**, 424–439.
- Tie, X. X., and P. Hess, 1997: The effects of volcanic eruption on the ozone mass exchange between the stratosphere and the troposphere. *J. Geophys. Res.*, **102**, 24 487–24 500.
- van Velthoven, P. F. J., and H. Kelder, 1996: Estimates of stratosphere–troposphere exchange: Sensivity to model formulation and horizontal resolution. *J. Geophys. Res.*, **101**, 1429–1434.
- Wei, M. Y., 1987: A new formulation of the exchange of mass and trace constituents between the stratosphere and the troposphere. *J. Atmos. Sci.*, **44**, 3079–3086.
- Wirth, V., 1996: Quasi-geostrophic dynamics of an upper tropospheric PV anomaly in two idealized high resolution models and related stratosphere–troposphere exchange. *Contrib. Atmos. Phys.*, **69** (2), 333–347.
- , and J. Egger, 1999: Diagnosing extratropical synoptic-scale stratosphere–troposphere exchange: A case study. *Quart. J. Roy. Meteor. Soc.*, **125**, 635–655.
- WMO, 1986: Atmospheric Ozone: 1985. Global Ozone Research and Monitoring Project Rep. 16, World Meteorological Organization, Geneva, Switzerland, 1090 pp.
- Yang, H., and K. K. Tung, 1996: Cross-isentropic stratosphere–troposphere exchange of mass and water vapor. *J. Geophys. Res.*, **101** (D5), 9413–9423.